Heliyon

ELSEVIER

Received:
23 September 2017
Revised:
4 January 2018
Accepted:
28 June 2018

Cite as: Dilli Ram Thapa, Xiaxin Tao, Feng Fan, Zhengru Tao. Aftershock analysis of the 2015 Gorkha-Dolakha (Central Nepal) earthquake doublet. Heliyon 4 (2018) e00678.
doi: 10.1016/j.heliyon.2018.e00678

Aftershock analysis of the 2015 Gorkha-Dolakha (Central Nepal) earthquake doublet

Dilli Ram Thapa [a,*], **Xiaxin Tao** [a,b], **Feng Fan** [a], **Zhengru Tao** [b]

[a] *School of Civil Engineering, Harbin Institute of Technology, Harbin 150090, China*

[b] *Institute of Engineering Mechanics, China Earthquake Administration, Harbin 150080, China*

[*] Corresponding author. Present address: Birendra Multiple Campus, Tribhuvan University, Nepal.

E-mail address: dilliramthapa14@hotmail.com (D.R. Thapa).

Abstract

On 25 April 2015, a large earthquake with moment-magnitude (M_w) 7.8 occurred at Gorkha (latitude 28.23° N and longitude 84.73° E) in Central Nepal. Just 17 days later, another large earthquake of M_w 7.3 occurred at Dolakha (latitude 27.80° N and longitude 86.06° E), about 140 km away from the previous epicenter. In this study, we deal with the aftershocks of these two earthquakes that occurred in the region (27°−28.5°N, 84°−87°E) spanning the period from 25 April 2015 to 28 May 2016 to find the spatiotemporal distribution patterns, the size distribution (*b*-value), and the aftershock decay rate (*p*-value) of this sequence. Aftershock epicenters of the 2015 Gorkha-Dolakha earthquake doublet are distributed over an area approximately 170 km in length and 70 km in width and largely confined in a depth range from 5 to 25 km. The spatial distribution of epicenters and known geological structures in this study reveals that aftershocks are limited on the east by the surface trace of the Everest lineament and on the south side by the surface trace of the segment of the Main Boundary Thrust (MBT). The estimated *b*-and *p*-values of this seismic sequence are 0.93 ± 0.03 and 0.79 ± 0.24, respectively. This *b*-value is higher than the *b*-value estimated by the previous studies, while the *p*-value corresponds in general with the *p*-value obtained by recent study in the region.

Keywords: Earth sciences, Natural hazards

https://doi.org/10.1016/j.heliyon.2018.e00678

1. Introduction

On 25 April 2015, a large earthquake with moment-magnitude (M_w) 7.8 occurred in Gorkha district (latitude 28.23° N and longitude 84.73° E) of central Nepal (hereafter referred to as the Gorkha earthquake) at about 32-km east of Lamjung district and about 80-km northwest of Kathmandu. Just 17 days later, another large earthquake of M_w 7.3 occurred on 12 May 2015 in Dolakha district (latitude 27.80° N and longitude 86.06° E) farther eastward (hereafter referred to as the Dolakha earthquake) at about 140-km east of the Gorkha earthquake, as shown in Fig. 1. These two large events and associated aftershocks caused many casualties (>8500 deaths), injuries (>22,000), damage (>5 million houses) and economic losses (~7 billion US dollars) in the country (Government of Nepal, 2015). Both earthquakes are occurred in the central segment of a Himalaya collided zone between the Eurasia Plate and the Indian Plate (Bilham, 2015). The ongoing collision of Eurasia-Indian plates governing the present day seismotectonics of the region that is expressed by the existence of active faults and lineaments (Nakata, 1972, 1982, 1989; Armijo et al., 1986; Dasgupta et al., 1987; Nakata and Kumahara, 2002; Taylor and Yin, 2009) and the occurrence of large earthquakes in the past (Thapa and Wang, 2013; Thapa et al., 2017).

Both these earthquakes are the two large well-recorded events occurred in Nepal since the 1934 Nepal-Bihar catastrophic earthquake ($M_w = 8.4$). Seismicity history of Nepal (Thapa and Wang, 2013; Thapa et al., 2017) shows that earthquakes of such large magnitudes are common in the country and one slightly smaller magnitude

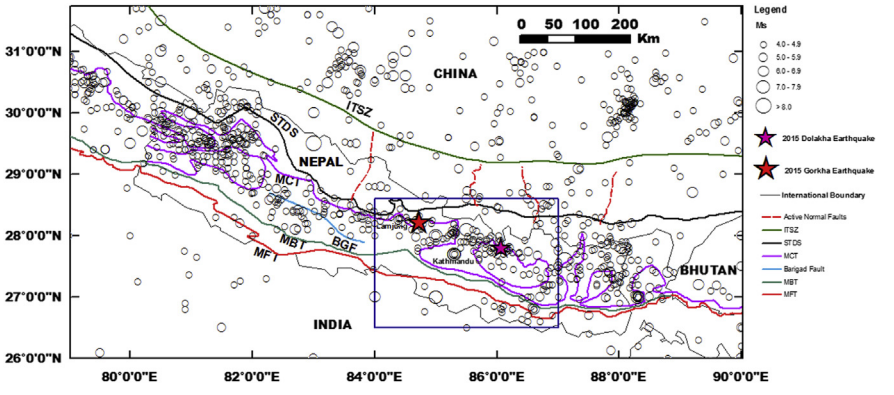

Fig. 1. Major faults and distribution of earthquakes in Nepal and the surrounding region. ITSZ-Indus Tsangpo Suture Zone; STDS-South Tibetan Detachment System; MCT - Main Central Thrust; BGF - Bari Gad Fault; MBT - Main Boundary Thrust; and MFT - Main Frontal Thrust. ITSZ; MCT; BGF; MBT; MFT and active normal faults (Red discontinuous lines) modified from Thapa et al. (2017), STDS modified from Hodges (2000). Epicenter locations of earthquakes (black circles) from 1255 to 24 April 2015 are taken from Thapa et al. (2017). Stars are the epicenters of the 2015 Gorkha and Dolakha earthquakes.

https://doi.org/10.1016/j.heliyon.2018.e00678

event ($M_w = 7.7$, 1833) than the Gorkha earthquake had occurred in an area between the 2015 Gorkha and the Dolakha main shocks. The recent 2015 two earthquakes were followed by a large number of aftershocks, including three events with moment-magnitudes equal to and greater than 6.3 ($M_w = 6.6$, 25 April 2015; $M_w = 6.7$, 26 April 2015; $M_w = 6.3$, 12 May 2015).

As known, aftershocks associated with strong earthquakes give information related to the earth's crust, hence the analysis of aftershocks has become a more common research topic in recent years. Statistical approaches (i.e., the Gutenberg-Richter frequency-magnitude relationship and the modified Omori law/Omori-Utsu law) are often employed for the study of aftershocks. Over the last four decades, several studies have primarily attempted to analyze the aftershocks of individual earthquakes worldwide (e.g., Stephens et al., 1980; Hauksson et al., 1995; Utsu et al., 1995; Guo and Ogata, 1997; Ogata, 1999; Hamburger et al., 2011). These investigations have provided the space-time as well as depth characteristics of the aftershocks. In the context of Nepal, several studies (Adhikari et al., 2015; Ogata and Tsuruoka, 2016; Ichiyanagi et al., 2016) have attempted to provide the account of aftershocks of the 2015 Gorkha earthquake. These studies considered the Dolakha earthquake as the largest aftershock of the Gorkha earthquake, no matter a theoretically conflicting that the magnitude of the Dolakha earthquake was not in accordance with the Båth's law, which stated that the size difference between the main shock and largest aftershock typically lies within a range of 1.1−1.2 magnitude units (Båth, 1965).

Although the longitudinal and transverse faults as well as lineaments have been identified in Central Nepal and the surrounding region (Nakata, 1972, 1982, 1989; Nakata and Kumahara, 2002; Dasgupta et al., 1987; Taylor and Yin, 2009) and some aftershocks studies of the 2015 earthquakes have been carried out (e.g., Adhikari et al., 2015; Ichiyanagi et al., 2016; Ogata and Tsuruoka, 2016), no studies have attempted to investigate the spatial relationship between the surface trace of known faults as well as lineaments and epicenter distribution of aftershocks and to analyze aftershocks considering two earthquakes as an earthquake doublet. Here, we consider these two earthquakes as an earthquake doublet (hereafter referred to as the Gorkha-Dolakha doublet) and analyze their aftershocks and the above mentioned spatial relationship.

The aim of this study is to investigate the aftershocks of the Gorkha-Dolakha earthquake doublet occurring in the region (27°−28.5°N, 84°−87°E) from 25 April 2015 to 28 May 2016. For this purpose, we analyze and present the spatiotemporal distribution patterns, the size distribution (*b*-value), and the aftershock decay rate (*p*-value). The analysis result enables us to improve our understanding of the aftershock evolution of this part of Nepal.

https://doi.org/10.1016/j.heliyon.2018.e00678

2. Methodology

The primary problem of seismicity analysis, especially for the aftershock analysis is to choose an appropriate spatial and temporal range for statistics. In this study, we compiled the aftershocks occurred in the geographic window between 27°−28.5°N and 84°−87°E for the period between 25 April 2015 and 28 May 2016 from the United States National Earthquake Information Centre (NEIC), since the occurrence rate and magnitudes of the aftershocks outside the area in the same time period and in the same area outside the time period are both obviously much less and smaller than those selected. This aftershock dataset contains 298 aftershocks with body wave magnitudes equal to or greater than 4.0. It consists of 266 aftershocks between magnitude 4.0 and 4.9, 28 aftershocks between magnitude 5.0 and 5.9, and four between magnitude 6.0 and 6.9.

To analyse this aftershock sequence quantitatively, we adopted two most commonly and widely well-known scaling laws, namely, the Gutenberg-Richter frequency-magnitude relation (Gutenberg and Richter, 1944) and the Modified Omori's Law/Omori-Utsu law (Utsu, 1961). The Gutenberg-Richter law that best characterizes the power-law size distribution of earthquakes can be expressed here below in Equation (1):

$$log_{10}N(M) = a - bM \tag{1}$$

in which N is the cumulative number of earthquakes with magnitude equal to or greater than magnitude M, and a and b represent the empirical constants of the law. The a and b values in this study are estimated using the least squares regression method considering that the USGS earthquake catalogue is complete with body wave magnitudes equal to or greater than 4.0.

Scaling law that is adopted to estimate the decay rate of aftershocks associated with a major event was initially described more than two-century ago by Omori (1884). The original Omori law (1884) is given here in the following equation:

$$n(t) = \frac{K}{(c+t)} \tag{2}$$

in which $n(t)$ is the occurrence rate of aftershocks in time period t, and K and c are empirical constants (Omori, 1884). During the early-sixties of the last century, Utsu (1961) extended the original Omori law, which is now called as the modified Omori's Law. The well-established modified Omori's Law commonly used in statistical seismology for characterizing the temporal decay process of the occurrence rate of aftershocks sequence can be expressed as (Utsu, 1961; Utsu et al., 1995):

https://doi.org/10.1016/j.heliyon.2018.e00678

$$n(t) = \frac{K}{(c+t)^p} \tag{3}$$

where p is an additional constant and other remaining notations are the same as above in Equation (2). In this study, the modified Omori law parameters are estimated using the exponential fitting from aftershocks datasets described above.

3. Results and discussion

3.1. Spatial and temporal distribution of aftershocks

The distribution of aftershock epicenters in the region from 25 April 2015 to 28 May 2016 is shown in Fig. 2. The figure demonstrates that aftershocks of the Gorkha earthquake are mostly distributed to the southeast of the main shock epicenter and aftershocks following the Dolakha earthquake located mainly between the two main shocks and some to the southeast of the Dolakha main shock. Two strong early aftershocks ($M_w = 6.6$, 25 April 2015; $M_w = 6.7$, 26 April 2015) are close to the Gorkha main shock, whereas the Dolakha main shock and its strong aftershock event ($M_w = 6.3$, 12 May 2015) are at the easternmost extremity of the aftershock zone of the Gorkha quake. Following the Dolakha main shock, the primary aftershock area expanded 20 km more to the east. Thus, the total extent of the aftershocks area became approximately 170 km in length by 70 km in width in a nearly southeast-northwest trending direction. This aftershock zone encompasses the rupture areas

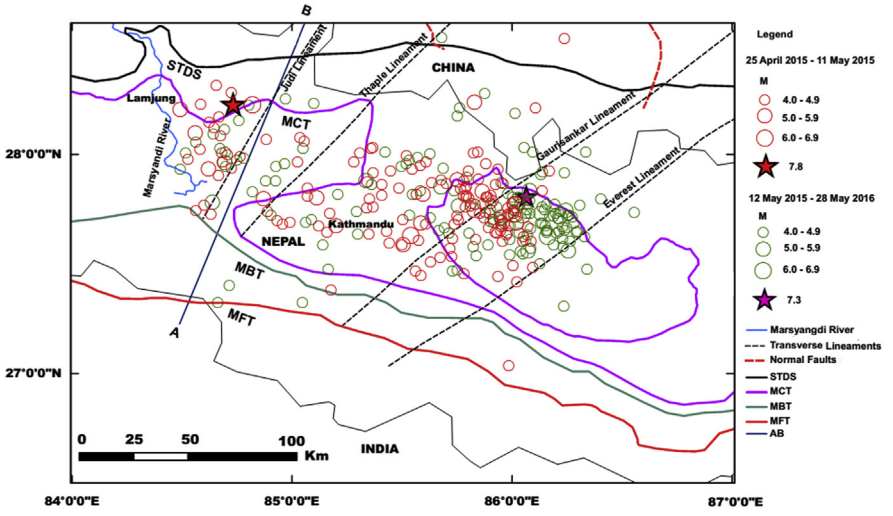

Fig. 2. Epicenter Map of the 2015 Gorkha and Dolakha earthquakes, aftershocks, and major faults in the study area. AB is the location of the cross section shown in Fig. 4. Transverse faults/lineaments (Black discontinuous lines) modified from Dasgupta et al. (1987) and other faults legend is the same as in Fig. 1. Stars are the epicenters of the 2015 Gorkha and Dolakha earthquakes. Red and green circles are the epicenters of aftershocks occurring between 25 April 2015 and 11 May 2015, 12 May 2015 and 28 May 2016, respectively.

https://doi.org/10.1016/j.heliyon.2018.e00678

of the earthquake doublet (Fan and Shearer, 2015) and is largely bounded on the west side by the Marsyangdi river, on the east by the surface trace of the Everest lineament and on the south side by the surface trace of the active segment of the Main Boundary Thrust (MBT). Both the Everest lineament and the segment of the MBT lies in this aftershock zone are previously recognized to be active geological structures (Nakata, 1972, 1982, 1989; Dasgupta et al., 1987), whereas the transverse features and the related tectonic structures along the Marsyangdi River and its tributaries are still unknown. Further detail research is necessary to clarify the existence/non existence of active tectonic features in the Marsyangdi valley.

Fig. 3 illustrates the time-magnitude distribution of aftershocks of the 2015 Gorkha-Dolakha earthquake doublet. It can be seen from the figure that two of the three strongest ($M_w = 6.6$, 25 April 2015; $M_w = 6.7$, 26 April 2015) aftershocks occurred within 2 days after the Gorkha main shock. A significant number of aftershocks are observed within this 2 days time period and then the aftershock activity decayed during the first 17 days till the Dolakha earthquake occurred on 12 May 2015 at 12:50 Kathmandu Time (07:05 UTC). The Dolakha main shock produced its own aftershocks, including the strong event ($M_w = 6.3$) that occurred within 31 minutes after the Dolakha quake on the same day at 13:21 Kathmandu Time (07:36 UTC). It was also followed by a productive number of aftershocks that resulted almost doubling the earthquake sequence. In sum, the significant number of aftershocks occurred within the first 2−3 months after the main shocks then the activity in the sequence gradually decaying over the whole study period.

Fig. 4 shows the distribution of the Gorkha-Dolakha earthquake doublet and their aftershocks on a northeast (N20°E) striking cross section (A and B). It can be observed from the figure that the overwhelming majority of the aftershocks occurred between 5 and 25 km deep and a small number of events extending down to 25 km depth. The depth section also shows that the maximum depth of aftershocks of this sequence in Central Nepal generally decreases from north to south.

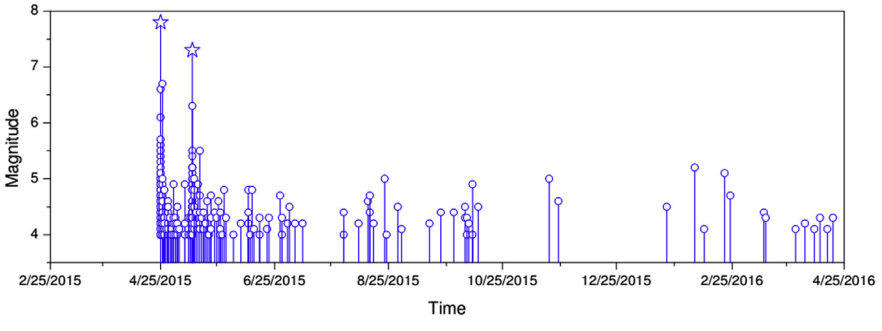

Fig. 3. Magnitude versus time for aftershocks ($M_b \geq 4.0$) occurring between 25 April 2015 and May 2016 associated with the 2015 Gorkha-Dolakha earthquake doublet in central Nepal. Stars are the 2015 Gorkha and Dolakha earthquakes.

https://doi.org/10.1016/j.heliyon.2018.e00678

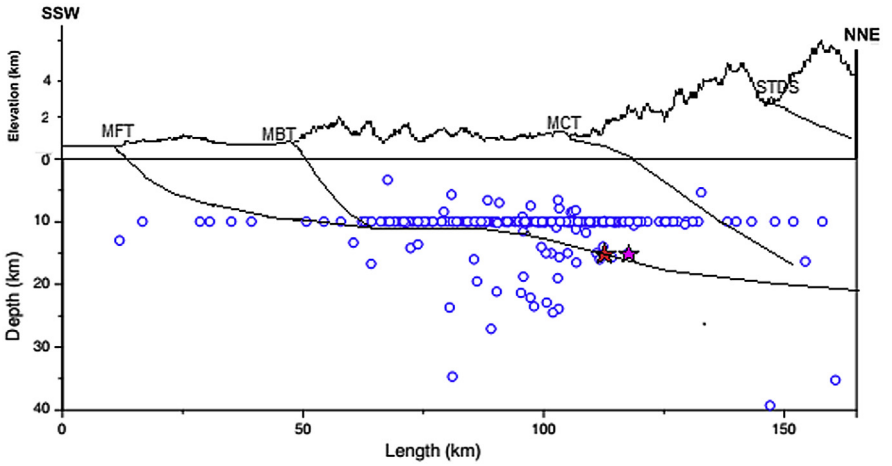

Fig. 4. Northeast (N20°E) striking cross section showing the Gorkha and Dolakha earthquake doublet and aftershocks (blue open circles). Stars on the left and right are the Gorkha and Dolakha earthquakes, respectively.

3.2. Magnitude-frequency distribution and decay rate of the aftershocks

The earthquake number-size distribution with *b*-value and the aftershock decay rate (*p*-value) of the sequence has been estimated by means of the magnitude-frequency relation of Gutenberg and Richter given in Equation (1) and the modified Omori law given in Equation (3), respectively. The results of the analysis are presented in Figs. 5 and 6.

Fig. 5 shows the magnitude-frequency distribution of aftershocks for the Gorkha-Dolakha earthquake doublet. The small blue squares indicate the actual number of

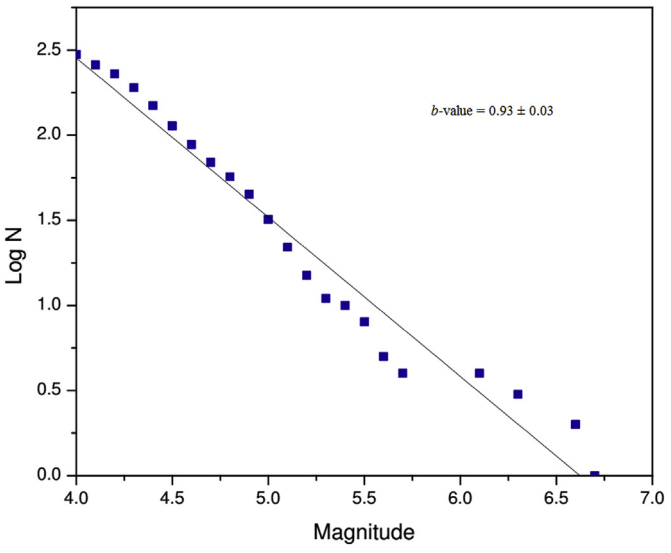

Fig. 5. Magnitude-frequency distribution of aftershocks ($M_b \geq 4.0$) of the 2015 Gorkha-Dolakha earthquake doublet.

https://doi.org/10.1016/j.heliyon.2018.e00678

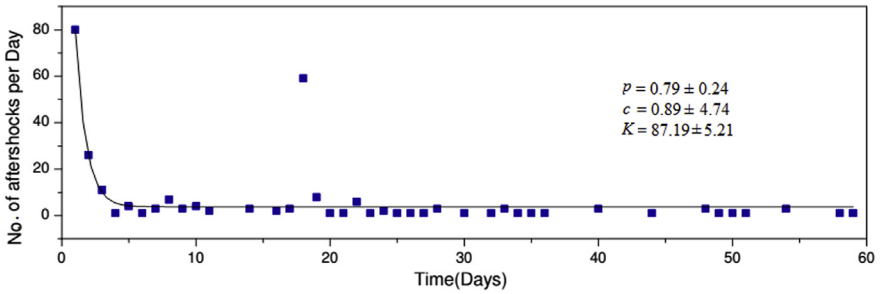

Fig. 6. The modified Omori fitting of aftershocks ($M_b \geq 4.0$) occurring within 60 days of the 2015 Gorkha-Dolakha earthquake doublet.

aftershocks with magnitudes no less than the corresponding magnitude and the line is fitted with *b*-value (0.93 ± 0.03), in the figure. This *b*-value is higher than the value of 0.80 ± 0.05 estimated by Adhikari et al. (2015) from aftershocks with local magnitude greater than 4.0 occurring within the first 45 days of the sequence considering the 12 May Dolakha main shock as a largest aftershock. This high *b*-value is associated on one hand with the dominance proportion of small size events in our aftershock datasets for a year longer time period. It is worth noting on the other hand that the magnitude-frequency distribution curve would be different if we consider the Dolakha earthquake as a largest aftershock of the Gorkha earthquake. The *b*-value slope would be flatten if we added the $M_w = 7.3$ event in the aftershock dataset. That dataset would be inadequate to obtain the good *b*-value statistics since the M_w 7.3 point is quite different from the fitted magnitude-frequency line. The result of this paper shows that the *b*-value of aftershocks of an earthquake doublet must be higher than that of a single main shock.

Fig. 6 displays the occurrence rate of aftershocks occurring within 60 days of the Gorkha-Dolakha earthquake doublet. One can see from the figure that the occurrence rate decayed very fast in the first 7 days, and then decayed gradually within 60 days afterwards. The data points in the figure also shows that the Dolakha quake occurred 17 days after the first main shock is far away from the curve; but does not disturb the decaying process. The parameters of the Omori's law primarily vary with the tectonic environment (e.g., styles of faulting) of the region (Tahir and Grasso, 2015). The estimated *p*-value in this study 0.79 ± 0.24, is very close to the value 0.80 ± 0.4 estimated by Adhikari et al. (2015) for the 2015 main cluster and is slightly lower than that of Tahir and Grasso (2015) who obtained p-value 0.82 ± 0.02 for the thrust faulting. The result of the present study shows that p-value of an earthquake doublet seems to be similar with that of a single main shock.

In a nutshell, the Dolakha earthquake must not be considered as an aftershock of the Gorkha shock for the magnitude-frequency analysis, but does not appears to affect the analysis of the decay rate of aftershocks. Doublet seismic events are well-documented in the recent seismological literature (e.g., Gibowicz and Lasocki, 2005; Vallée and Di Luccio, 2005; Karakostas et al., 2015). It is thus concluded

https://doi.org/10.1016/j.heliyon.2018.e00678

that these two 2015 earthquakes occurred in Nepal should be considered as an earthquake doublet and aftershocks must be analyzed as those of an earthquake doublet.

4. Conclusions

Aftershocks of the Gorkha-Dolakha earthquake doublet occurred in the region (27°−28.5°N, 84°−87°E) from 25 April 2015 to 28 May 2016 are analyzed and their spatiotemporal distribution patterns, the size distribution (*b*-value), and the aftershock decay rate (*p*-value) are estimated. This analysis clearly shows that aftershocks are distributed over an area of approximately 170 km in length by 70 km in width in a nearly southeast-northwest trending direction and confined to a depth between 5 and 25 km. The analysis also shows that there is a significant number of aftershocks occurred within the first 2−3 months after the main shocks and the activity in the sequence gradually decayed over the entire study period. The *b*-value and *p*-value are 0.93 ± 0.03 and 0.79 ± 0.24, respectively. The *b*-value is higher than the value of 0.80 ± 0.05 estimated by Adhikari et al. (2015) for the 2015 sequence, whereas the *p*-value is very close to the value of 0.80 ± 0.4 as estimated by Adhikari et al. (2015) for the 2015 main cluster. The result of this paper indicates that the Gorkha and Dolakha earthquakes should consider as an earthquake doublet in the study of the magnitude-frequency relation of aftershocks, whereas this approximation does not seems to affect on the analysis of the rate of decay.

Finally, it is worth mentioning that the aftershock zone largely bordered in the west by the Marsyangdi river, in the south by the surface trace of the active segment of the MBT and in the east by the surface trace of the Everest lineament. The MBT and Everest lineament are known geological structures, whereas the transverse features and associated tectonic structures along the Marsyangdi river and its tributaries are still unknown. Further extensive research is necessary to clarify whether active tectonic features exists or not in the Marsyangdi valley.

Declarations

Author contribution statement

Dilli Ram Thapa: Conceived and designed the analysis; Analyzed and interpreted the data; Contributed analysis tools or data; Wrote the paper.

Xiaxin Tao: Conceived and designed the analysis; Analyzed and interpreted the data.

Feng Fan and Zhengru Tao: Analyzed and interpreted the data.

https://doi.org/10.1016/j.heliyon.2018.e00678

Funding statement

This work was supported by Scientific Research Fund of Institute of Engineering Mechanics, China Earthquake Administration (Grant No. 2017B12); and funds of 51478443, 51678540, 51178435 and 51778197 of National Nature Science Foundation of China.

Competing interest statement

The authors declare no conflict of interest.

Additional information

No additional information is available for this paper.

Acknowledgements

We thank the editor and associate editor for their editorial assistance. Reviews by E. Papadimitriou and Ch. Kourouklas have been significantly useful in improvement the manuscript.

References

Adhikari, L.B., Gautam, U.P., Koirala, B.P., Bhattarai, M., Kandel, T., Gupta, R.M., Timsina, C., Maharjan, N., Maharjan, K., Dahal, T., Hoste-Colomer, R., Cano, Y., Dandine, M., Guilhem, A., Merrer, S., Roudil, P., Bollinger, L., 2015. The aftershock sequence of the 2015 April 25 Gorkha-Nepal earthquake. Geophys. J. Int. 203, 2119−2124.

Armijo, R., Tapponnier, P., Mercier, J.L., Tonglin, H., 1986. Quaternary extension in Southern Tibet. J. Geophys. Res. 91, 13,803−13,872.

Båth, M., 1965. Lateral inhomogeneities of the upper mantle. Tectonophysics 2 (6), 483−514.

Bilham, R., 2015. Seismology: raising Kathmandu. Nat. Geosci. 8 (8), 582−584.

Dasgupta, S., Mukhopadhyay, M., Nandy, D.R., 1987. Active transverse features in the central portion of the Himalaya. Tectonophysics 136, 255−264.

Fan, W.Y., Shearer, P.M., 2015. Detailed rupture imaging of the 25 April 2015 Nepal earthquake using teleseismic P waves. Geophys. Res. Lett. 42, 5744−5752.

Government of Nepal, 2015. Nepal earthquake 2015: post disaster needs assessment. In: Key Findings, (Vol. A). National Planning Commission, Nepal.

https://doi.org/10.1016/j.heliyon.2018.e00678

Gibowicz, S.J., Lasocki, S., 2005. Earthquake doublets and multiplets in the Fiji-Tonga-Kermadec region. Acta Geophys. Pol. 53, 239–274.

Guo, Z., Ogata, Y., 1997. Statistical relation between the parameters of aftershocks in time, space and magnitude. J. Geophys. Res. 102 (B2), 2857–2873.

Gutenberg, B., Richter, C.F., 1944. Frequency of earthquakes in California. Bull. Seismol. Soc. Am. 34, 185–188.

Hamburger, M.W., Shoemaker, K., Horton, S., DeShon, H., Withers, M., Pavlis, G.L., Sherrill, E., 2011. Aftershocks of the 2008 Mt. Carmel, Illinois, earthquake; evidence for conjugate faulting near the termination of the Wabash Valley fault system. Seismol. Res. Lett. 82 (5), 735–747.

Hauksson, E., Jones, L.M., Hutton, K., 1995. The 1994 Northridge earthquake sequence in California: seismological and tectonic aspects. J. Geophys. Res. 100, 12,335–12,355.

Hodges, K.V., 2000. Tectonics of the Himalaya and southern Tibet from two perspectives. Geol. Soc. Am. Bull. 112, 324–350.

Ichiyanagi, M., Takai, N., Shigefuji, M., Bijukchhen, S., Sasatani, T., Rajaure, S., Dhital, M.R., Takahashi, H., 2016. Aftershock activity of the 2015 Gorkha, Nepal, earthquake determined using the Kathmandu strong motion seismographic array. Earth Planets Space 68, 25.

Karakostas, V., Papadimitriou, E., Mesimeri, M., Gkarlaouni, C.H., Paradisopoulou, P., 2015. The 2014 Kefalonia doublet (Mw6.1 and Mw6.0) central Ionian Islands, Greece: seismotectonic implications along the Kefalonia transform fault zone. Acta Geophys. 63, 1–16.

Nakata, T., 1972. Geomorphic history and crustal movements of foothills of the Himalaya. Sci. Rep. 22, 39–177. Tohoku University.

Nakata, T., 1982. A photogrammetric study on active faults in the Nepal Himalayas. J. Nepal Geol. Soc. 2, 67–80.

Nakata, T., 1989. Active faults of the Himalayas of India and Nepal. Geol. Soc. Am. Spec. Pap. 232, 243–264.

Nakata, T., Kumahara, Y., 2002. Active faulting across the Himalaya and its significance in the collision tectonics. Act. Fault Res. 22, 7–16.

National Earthquake Information Center (NEIC), United States Geological Survey, U.S.A, (http://neic.usgs.gov).

Omori, F., 1884. On the aftershocks of earthquakes. J. Coll. Sci. 7, 111–200.

https://doi.org/10.1016/j.heliyon.2018.e00678

Ogata, Y., 1999. Seismicity analysis through point-process modelling: a review. Pure Appl. Geophys. 155, 471−507.

Ogata, Y., Tsuruoka, H., 2016. Statistical monitoring of aftershock sequences: a case study of the 2015 Mw 7.8 Gorkha, Nepal, earthquake. Earth Planets Space 68, 44.

Stephens, C.D., Lahr, J.C., Fogleman, K.A., Horner, R.B., 1980. The St. Elias, Alaska, earthquake of 28 February 1979: regional recording of aftershocks and short-term pre-earthquake seismicity. Bull. Seismol. Soc. Am. 70, 1607−1633.

Tahir, M., Grasso, J.R., 2015. Faulting style controls for the space-time aftershock patterns. Bull. Seismol. Soc. Am. 105, 2480−2497.

Taylor, M.H., Yin, A., 2009. Active structures of the Himalayan-Tibetan orogen and their relationships to earthquake distribution, contemporary strain field, and Cenozoic volcanism. Geosphere 5 (3), 199−214.

Thapa, D.R., Wang, G., 2013. Probabilistic seismic hazard analysis in Nepal. Earthq. Eng. Eng. Vib. 12 (4), 577−586.

Thapa, D.R., Tao, X., Wang, G., Fan, F., 2017. Deterministic seismic hazard assessment for Nepal. In: 16th World Conference on Earthquake Engineering (16WCEE-2017, Paper No. 730), Santiago, Chile.

Utsu, T., 1961. A statistical study of the occurrence of aftershocks. Geophys. Mag. 30, 521−605.

Utsu, T., Ogata, Y., Matsuura, R.S., 1995. The centenary of the Omori formula for a decay law of aftershock activity. J. Phys. Earth 43, 1−33.

Vallée, M., Di Luccio, F., 2005. Source analysis of the 2002 Molise, southern Italy, twin earthquakes (10/31 and 11/01). Geophys. Res. Lett. 32, L12309.

 https://doi.org/10.1016/j.heliyon.2018.e00678